Design Of An ISS-Based Adaptive Controller For A Single-Phase Voltage Source Inverter

Viet-Hoang Nguyen[1], Van-Dat Quan[1], Van-Hoang Truong[1], Duy-Thai Ha[1,2], and Phuong Vu[1*]

[1] School of Electrical and Electronic Engineering, Ha Noi University of Science and Technology, Hanoi, Viet Nam
[2] Department of Electrical and Electronic Engineering, Faculty of Engineering and Technology, Hung Vuong University (HVU), Phu Tho, Vietnam
[*] Corresponding author. E-mail: phuong.vuhoang@hust.edu.vn

Received: Jan. 16, 2026; Accepted: Jul. 15, 2026

This paper presents a novel control approach based on input-to-state stability (ISS) for a single-phase voltage source inverter (VSI). The ISS-based adaptive controller is capable of mitigating the adverse effects of load disturbances that commonly arise in sliding mode control (SMC) schemes, while delivering superior output control performance. However, the application of ISS theory to controller design has not been extensively investigated, mainly due to the difficulty in selecting an appropriate ISS-Lyapunov function (ISS-LF). Therefore, in addition to detailing the controller design procedure, this paper also presents the theoretical basis for ISS-LF selection by combining the Backstepping method with adaptive control. The proposed approach is validated through simulations and experiment. The results demonstrate that the proposed control strategy achieves good performance for the considered system, including fast dynamic response, absence of transient error, global stability, and low THD of the output voltage.

Keywords: Input-to-state; VSI; Lyapunov stability; ISS-based adaptive controller

http://dx.doi.org/10.6180/jase.202611_34.041

1. Introduction

With the rapid development of renewable energy sources, inverter-related research has attracted significant attention in recent years. Among various inverter topologies, the single-phase voltage source inverter (VSI) has been widely employed in numerous applications such as uninterruptible power supplies (UPS), microgrids, and other automation systems [1–3]. To meet the increasingly stringent requirements on output voltage quality such as low voltage sag, low total harmonic distortion (THD), and satisfactory operation under both linear and nonlinear loads-the development of advanced control strategies for VSIs has become a widely studied research topic.

A variety of control methods have been proposed for VSI systems, including conventional linear control approaches such as PID control [4, 5], PR control [6, 7]. However, these methods suffer from inherent limitations. PID controllers are not well suited for the regulation of alternating signals, while PR controllers, although addressing this drawback, still share the common limitations of linear control schemes. In particular, their performance degrades under nonlinear load conditions, often resulting in unsatisfactory THD levels and voltage fluctuations during load variations [8]. These issues mainly arise because disturbance terms are commonly neglected during the modeling stage to simplify controller design, leading to unmodeled disturbances that adversely affect voltage quality. Disturbance observer-based (DOB) ap- proaches have been introduced to address this problem, but their effectiveness remains limited [9, 10].

The design of nonlinear controllers is commonly associated with stability criteria, among which Lyapunov stability is the most widely used, either in sliding mode control (SMC) applications or directly as a basis for controller synthesis. Reference [11] presents an adaptive Lyapunov-based control design; however, this controller suffers from mathematical limitations because it still depends on load-related terms. As a result, the reported simulation results are valid only for purely resistive loads. Moreover, the control signal generated by this approach lacks sufficient accuracy, which prevents its practical implementation and experimental validation. Reference [12] presents an alternative transformation approach for constructing a Lyapunov-based controller; however, it still fails to overcome the issue of dependence on load-related terms.

SMC is a robust nonlinear control approach that has been widely investigated. SMC is designed to completely reject disturbances through appropriate selection of the sliding surface and control law, thereby achieving desirable control performance [13, 14]. Nevertheless, chattering caused by highfrequency oscillations around the sliding surface remains a major drawback of SMC. This issue has been alleviated by various reaching law designs, such as Gao's reaching law, the single-power reaching law, and the exponential-based bi-power reaching law,... [15–17] Although these approaches have demonstrated good performance in both simulations and experiments, they still exhibit limitations in terms of mathematical rigor when load disturbances are present, resulting in incomplete analytical treatment. Disturbance compensation and estimation techniques based on DOB have been proposed as potential solutions [18], however, they do not completely eliminate disturbance terms in the mathematical derivations.

An alternative approach that has the potential to overcome the limitations of SMC, yet has not been widely applied to VSI control design, is based on the input-to-state stability (ISS) framework [19–23]. ISS has emerged as one of the most widely used frameworks for analyzing robust stability in the presence of external disturbances and modeling uncertainties. A broad range of ISS conditions has been established for various classes of dynamical systems, and these conditions are often expressed in terms of Lyapunov functions (LFs). Such functions are required to satisfy global properties, including positive definiteness, differentiability, and radial unboundedness, as well as appropriate conditions on their time derivatives along the trajectories of the nonlinear system, such as negative definiteness. The main challenge of this approach lies in constructing a Lyapunov function that fulfills all these requirements for a given system. The construction of a Lyapunov function for ISS analysis is generally more demanding than that for asymptotic stability in the absence of disturbances. In particular, a Lyapunov function that is suitable for the unperturbed system may fail to satisfy the additional conditions required for robustness analysis [24].

In this study, an ISS-based adaptive control design for a single-phase VSI is proposed by integrating the Backstepping technique [25–28] with the nonlinear damping theory presented in [29, 30], because Backstepping is typically applied to controller design for systems without uncertainties or with known uncertainties; therefore, it is necessary to combine it with nonlinear damping. Based on this framework, the control input for the VSI can be systematically derived, leading to an adaptive controller that guarantees Lyapunov stability. Simulation and experimental results demonstrate that the proposed ISS-based adaptive controller achieves performance comparable to SMC, while providing a more rigorous mathematical formulation due to the absence of explicit load disturbance terms in the control law.

In summary, the main contributions of this paper are as follows:

1. A comprehensive integration of ISS theory, nonlinear damping, and Backstepping to propose a new novel ISS-based adaptive control design methodology.
2. A new systematic procedure for constructing an ISS-Lyapunov function and applying it to VSI control, effectively eliminating the influence of uncertainties.
3. The proposed method is validated through both simulation and experimental studies. In simulation, two design approaches based on the Lyapunov stability criterion are compared with other methods to draw clear conclusions about the advantages and disadvantages of the proposed method.

2. Method

2.1. Preliminaries

The controller design problem based on the Lyapunov stability criterion, which incorporates disturbance rejection, was previously addressed in was addressed in, This approach utilizes an indirect adaptive method to mitigate the impact of disturbances by substituting the unknown disturbance terms with identifiable state variables through an estimation law. Indirect adaptive methods differ from direct adaptive methods. In direct adaptive, the control parameters are updated directly, or the disturbances are explicitly estimated. In contrast, indirect adaptive associates the estimated value with a function related to the

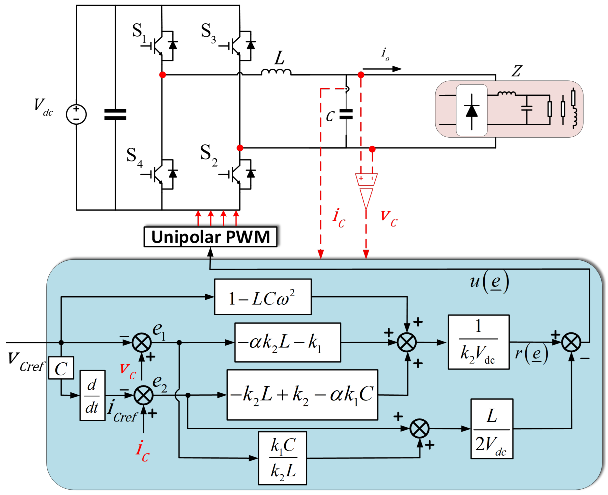

Fig. 1. Proposed ISS-based adaptive controller

state variable in the model and adjusts the control parameters, specifically the control law in [11] until this variable converges to zero. As a result, the estimate obtained via indirect adaptive does not necessarily match the actual value it represents.

According to the proposed ISS-based adaptive control structure shown in Fig. 1, the indirect adaptive control is implemented following a similar principle; the disturbance part in this case is Z , which is also called actual load impedance.

Although the control law is designed to eliminate the effect of the uncertain load, one of the conditions required for the Dual-loop Lyapunov-based controller to satisfy the Lyapunov stability criterion is not satisfied for all values of Z. When Z is a resistive load, the inequality is guaranteed. However, when Z includes inductive or capacitive components, its mathematical representation inherently involves a complex term of the form $j\omega$, making it no longer valid in this case. This limitation is also evident in [11], where the RL load scenario was not considered in the simulation study. When this controller is simulated with an RL load, the output voltage v_o becomes unstable. The corresponding results are presented and discussed in Section 3.

This demonstrates the significant consequences of insufficient mathematical rigor in the analysis. Similarly, the SMC controller presented in [16] is also subject to a similar issue. It can be observed that the load impedance Z still explicitly appears in model, undermining mathematical rigor in the parameter derivation. Although the experiment results in the study are not significantly affected, this issue may reduce the overall validity and theoretical consistency of the analysis.

The issue associated with the presence of an unknown disturbance term, as previously discussed, also arises in control strategies such as Backstepping. To address this limitation, the authors propose a controller design based on the ISS Lyapunov framework, which is specifically intended to handle systems with uncertain disturbances such as Z. Compared with existing ISS-based design approaches in [19, 23], proposed method enhances the conventional approach by synergizing the ISS framework with Backstepping, while employing control parameters optimized for the specific system. This combination enhances design flexibility and ensures that the necessary stability conditions are satisfied. As a result, the method achieves comparable control performance while maintaining robustness against disturbances. The detailed design procedure is presented below.

Consider the nonlinear system:

$$\frac{d\underline{x}}{dt} = f(\underline{x}, \underline{u}, \underline{d}), \forall \underline{x}(0) = \underline{x}_0 \tag{1}$$

First, consider system with $\underline{d} = 0$. Definition 3 in [20] introduces the fundamental concepts related to ISS, including the definition of an ISS system, the notion of local ISS, and the concept of a nonlinear asymptotic gain. Based on the conditions under which system Eq. (1) is ISS if $\forall t \geq 0$ we have:

$$\|\underline{x}(t, \underline{x}_0, \underline{d})\| \leq \beta(\|\underline{x}_0\|, t) + \gamma\left(\|\underline{d}\|_{[0,t]}\right) \tag{2}$$

By combining this with the condition in [19]: $\lim_{t\to\infty} \underline{x}(t, \underline{x}_0, \underline{d}) \leq \gamma\left(\|\underline{d}\|_{[0,t]}\right)$ the definition of an attractor can be derived as follows: $\underline{x}(t, \underline{x}_0, d)$ is bounded and arbitrarily close to a sphere whose radius is proportional. This set, referred to as the Attractor, is illustrated in Fig. 2.

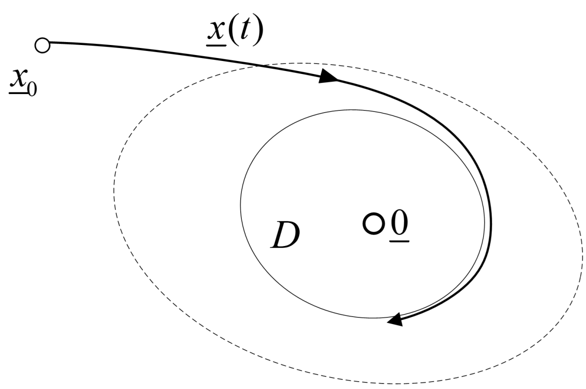

Fig. 2. Asymptotic gain property

The Attractor is defined in [29] according to the Lyapunov criterion. For ISS, the concept of the region of Attractor also exhibits similar properties. Inequality Eq. (2)

can be derived from the concept of the region of attraction as presented in Definition 4.7 in [31]. Specifically, if there exists a Lyapunov function $V(\underline{x})$, then its time derivative must be negative outside the attractor. This result plays an important role in determining the region of attraction, and establishing the global asymptotic stability of the ISS system for trajectories on or outside the attractor. After introducing the notion of ISS stability in Definition 3, Definition 6 [20] provides the framework for the ISSLyapunov function (ISS-LF) including its definition and the conditions under which a smooth function $V : \mathbb{R}^n \to \mathbb{R}_+$is called ISS-LF for the system Eq. (1) if there are $\gamma_1, \gamma_2, \gamma_3 \in \mathcal{K}_\infty$ and $\theta \in \mathcal{K}$ such that:

$$\gamma_1(\|\underline{x}\|) \leq V(\underline{x}) \leq \gamma_2(\|\underline{x}\|), \tag{3}$$

$$\frac{\partial V(\underline{x})}{\partial \underline{x}} f(\underline{x}, \underline{d}) \leq \theta(\|\underline{d}\|) - \gamma_3(\|\underline{x}\|) \tag{4}$$

By combining Definition 3 and Definition 6, the result stated in Theorem 2 [20] can be obtained.

The foregoing definitions and theorems are introduced to establish the fundamental concepts and conditions required for ISS. These theoretical results provide the mathematical foundation for the stability analysis of the controller design developed in the subsequent sections. Building upon this framework, the proposed control strategy is derived by integrating Sontag's approach with a Backstepping-based design methodology, while incorporating nonlinear damping techniques in design ISS-based adaptive controller to effectively attenuate disturbance effects.

Theorem 1 [21] makes a significant contribution to controller design. In particular, its proof establishes the conditions under which the system is stable when there exists a smooth control Lyapunov function (CLF) V, thereby guaranteeing the existence of a smooth stabilizer k. The combination of this theorem with Backstepping controller design theory constitutes the main novelty of the proposed method. The theoretical foundations of the Backstepping approach are presented in detail in Assumption 2.7 [29] and Lemma 2.8 [29].

At this stage, the design is completed only for system Eq. (1) in the absence of uncertainties. The objective is to develop a controller for the system: $\frac{dx}{dt} = f(\underline{x}, \underline{u}, \underline{d})$ with $\underline{d}(t)$ is uncertain nonlinearities. The requirement of the ISS-based adaptive control problem is to design a controller $\underline{u} = \underline{r}(\underline{x})$, such that the closed-loop system $\frac{dx}{dt} = f(\underline{x}, \underline{r}(\underline{x}), \underline{d})$ exhibits ISS-stable state trajectories.

To achieve this objective, it is necessary to further incorporate the nonlinear damping theory presented in Lemma 5.6 [29]. This lemma provides the key idea for designing an ISS-based adaptive controller for systems with uncertainties, and addresses the uncertainty by employing the concept of Attractor. By synthesizing the aforementioned theoretical results, an ISS-based adaptive controller design methodology can be formulated as follows:

Consider the system:

$$\frac{d\underline{x}}{dt} = \underline{f}(\underline{x}) + H(\underline{x})\underline{u} + G(\underline{x})\underline{d}(t) \tag{5}$$

with $\underline{d}(t)$ is uncertain nonlinearities, $\|\underline{d}\| \leq \|\underline{d}\|_\infty$ and: $H(\underline{x}) = (\underline{h}_1(\underline{x}), \ldots, \underline{h}_n(\underline{x}))\,; G(\underline{x}) = \left(\underline{g}_1(\underline{x}), \ldots, \underline{g}_m(\underline{x})\right)$

Theorem 1: System Eq. (5) has a controller that ensures global asymptotic stability (GAS), given as follows (with $k, p \geq 0$):

$$\underline{u} = \begin{cases} \underline{r}(\underline{x}) - k^p \frac{|\underline{c}(\underline{x})|^p}{|\underline{\alpha}(\underline{x})|^2} \underline{\alpha}(\underline{x}), & \underline{x} \notin Z \\ 0, & \underline{x} \in Z \end{cases}$$

Proof: Assume that $V(\underline{x})$ is CLF of $\frac{d\underline{x}}{dt} = \underline{f}(\underline{x}) + H(\underline{x})\underline{u}$, which means $V(\underline{x})$ is positive define, according to Lyapunov stability we have:

$$\begin{aligned} &\gamma_1(\|\underline{x}\|) \leq V(\underline{x}) \leq \gamma_2(\|\underline{x}\|), \quad \gamma_1, \gamma_2 \in \mathcal{K}_\infty \\ &\frac{\partial V}{\partial \underline{x}}[f(\underline{x}) + H(\underline{x}) r(\underline{x})] \leq -W(\underline{x}) \\ &\rho_1(\|\underline{x}\|) \leq W(\underline{x}) \leq \rho_2(\|\underline{x}\|), \quad \rho_1, \rho_2 \in \mathcal{K} \end{aligned} \tag{6}$$

The above condition is utilized in the subsequent stability proof, in conjunction with Young's and Hölder's inequalities. By applying the Backstepping method, we obtain CLF $V(\underline{x}) = V_1(\underline{x}) + \frac{1}{2}[\xi - r_1(\underline{x})]^2$. Following the Backstepping design principle and in combination with Theorem 1 [21], the statefeedback controller $r(\underline{x})$ is derived as:

$$\underline{r}(\underline{x}) = \begin{cases} -c\,(\xi - r_1(\underline{x})) - \frac{\partial V_1(\underline{x})}{\partial \underline{x}} \cdot H(\underline{x}) \\ \quad + \frac{\partial r_1(\underline{x})}{\partial \underline{x}}[f(\underline{x}) + H(\underline{x})\xi] & \text{for } \underline{x} \notin Z \\ \quad 0, & \text{for } \underline{x} \in Z \end{cases} \tag{7}$$

with $c > 0, r_1(\underline{x})$ is the controller of subsystem with CLF $V_1(\underline{x}), \xi$ is the virtual control input of subsystem, $\xi = r_1(\underline{x})$.

As presented above, the controller in Eq. (8) is constructed based on Sontag's Theorem, and the authors combine it with the Backstepping approach. To arrive at this result, it is necessary to establish and prove the relationship between Sontag's Theorem and Backstepping. First, Sontag considers a system of the following form: $\frac{dx}{dt} = \underline{f}(\underline{x}) + \underline{h}(\underline{x})\underline{u}$ and assume that V is a CLF for this system.

Let: $a(\underline{x}) := \frac{\partial V}{\partial \underline{x}} \cdot \underline{f}(\underline{x}), \quad b(\underline{x}) := \frac{\partial V}{\partial \underline{x}} \cdot \underline{h}(\underline{x})$
The condition that V is a CLF is equivalent to requiring that:

$$b(\underline{x}) = 0 \Rightarrow a(\underline{x}) < 0 \tag{8}$$

For every nonzero state $\underline{x}$, this implication ensures that $(a(\underline{x}), b(\underline{x}))$ is stabilizable when interpreted as a linear system with a single scalar input. As a result, a control law $u = k(\underline{x})$ can be constructed for the original nonlinear system such that V remains a CLF for the corresponding closed-loop dynamics. Hence, the theory guarantees that, given a CLF V, when $b(\underline{x}) = 0$ system is stabilizable, when $b(\underline{x}) \neq 0$, a feedback law $u = k(\underline{x})$ can be designed to achieve stability. The control law selected by Sontag, given by $u = -\frac{a+\sqrt{a^2+b^2}}{b}$ satisfied the condition $\frac{dV}{dt} = -\sqrt{a^2+b^2} < 0$. Based on this result, the relationship between Sontag's theorem and Backstepping can be established.

According to the Backstepping theory [29], function V that is a CLF for system : $\frac{dx}{dt} = f(\underline{x}) + h(\underline{x})\underline{u}$ which means it satisfied $dV/dt < 0$ for all $b(x)$. This conclusion can also be explained by Sontag's theorem: when $b(\underline{x}) = 0$ system is stabilizable, and when $b(\underline{x}) \neq 0$, the control law derived via Backstepping can stabilize the system. This shows a correspondence between Sontag's Theorem and Backstepping. Therefore, these two theories can be integrated, leading to the derivation of Equation Eq. (8).

Notation:

$$\underline{c}(\underline{x}) = \left(L_{\underline{g}_1}V, L_{\underline{g}_2}V, \ldots, L_{\underline{g}_m}V\right)^T \tag{9}$$

with $\underline{c}(\underline{x})$ is defined as the Lie derivative of the Lyapunov function V with respect to the disturbance vector fields. Thus, if there exists a constant $p > 1$ such that for all $\underline{x} \in Z$ we have:

$$L_{\underline{f}}V + \frac{1}{p}|\underline{c}(\underline{x})|^p \leq -\rho(\|\underline{x}\| \tag{10}$$

with ρ satisfied $\|\rho\|_\infty > \frac{1}{q}\|\underline{d}\|^q_{\infty,q}, q = \frac{p}{p-1}$. The conditions defined in Inequality Eq. (10) are selected to satisfy the ISS criteria, as demonstrated in the proof below. Then $V(\underline{x})$ is an ISS-LF and the corresponding ISS-based adaptive controller is:

$$\underline{u} = \begin{cases} \underline{r}(\underline{x}) - k^p \frac{|\underline{c}(\underline{x})|^p}{|\underline{\alpha}(\underline{x})|^2 p}\underline{\alpha}(\underline{x}), & \underline{x} \notin Z \\ 0, & \underline{x} \in Z \end{cases} \tag{11}$$

where $\underline{\alpha}(\underline{x}) = \left(L_{\underline{h}_1}V, L_{\underline{h}_2}V, \ldots, L_{\underline{h}_n}V\right)^T, Z = \{\underline{x} \in \mathbb{R}^n \| \underline{\alpha}(\underline{x}) |= 0\}, k > 0$ and $\underline{\alpha}(\underline{x})$ is defined as the Lie derivative of the Lyapunov function along the control vector fields. Equation Eq. (11) is a corresponding ISSbased adaptive controller.

Next, we determine the region of attraction of the above controller. Assume that $\underline{x} \in Z$, then along the state trajectories of the closed-loop system, we have:

$$\begin{aligned} \frac{dV}{dt} &= \frac{\partial V}{\partial \underline{x}}[f(\underline{x}) + H(\underline{x})\underline{u} + G(\underline{x})\underline{d}] \\ &= L_f V + \underline{c}^T\underline{d} \leq L_f V + \|\underline{c}\|\|\underline{d}\| \\ \Leftrightarrow \frac{dV}{dt} &\leq L_f V + \frac{1}{p}|\underline{c}|^p + \frac{1}{q}|\underline{d}|^q \end{aligned}$$

(Young's inequality)

$$\leq -\rho(\|\underline{x}\|) + \frac{1}{q}\|\underline{d}\|^q_\infty \tag{12}$$

Similarly, when $\underline{x} \notin Z$:

$$\underline{u}(\underline{x}) = \underline{r}(\underline{x}) - \frac{|\underline{c}(\underline{x})|^p k^p}{|\underline{\alpha}(\underline{x})|^2 p}\underline{\alpha}(\underline{x})$$

we also have:

$$\begin{aligned} \frac{dV}{dt} &= \frac{\partial V}{\partial \underline{x}}[f(\underline{x}) + H(\underline{x})\underline{u} + G(\underline{x})\underline{d}] \\ &= \frac{\partial V}{\partial \underline{x}}(f(\underline{x}) + H(\underline{x})\underline{r}) + \underline{c}^T\underline{d} - \frac{k^p}{p}|\underline{c}|^p \\ \Rightarrow \frac{dV}{dt} &\leq -W(\underline{x}) + \underline{c}^T\underline{d} - \frac{k^p}{p}|\underline{c}|^p \\ &\leq -W(\underline{x}) + \frac{k^p}{p}|\underline{c}|^p + \frac{1}{k^q q}\|\underline{d}\|^q - \frac{k^p}{p}|\underline{c}|^p \\ &\leq -W(\underline{x}) + \frac{1}{k^q q}\|\underline{d}\|^q_\infty \end{aligned} \tag{13}$$

Clearly, according to Definition 3 [20], both Inequalities Eq. (12) and Eq. (13) confirm the ISS stability of the closed-loop system consisting of plant Eq. (5) and controller Eq. (11) for all $\underline{x} \in \mathbb{R}^n$.

To determine the attractor D, we start from:

$$\frac{dV}{dt} \geq 0 \Rightarrow \|\underline{d}\|^q_\infty \geq \max\{\rho(\|\underline{x}\|)q, W(\underline{x})k^q q\}$$

and arrive to the sufficient condition:

$$\begin{aligned} &\|\underline{d}\|^q_\infty \geq \max\{\rho(\|\underline{x}\|)q, \rho_2(\|\underline{x}\|)k^q q\} \\ &\|\underline{x}\| \leq \max\left\{\rho^{-1}\left(\frac{\|\underline{d}\|^q_\infty}{q}\right), \rho_2^{-1}\left(\frac{\|\underline{d}\|^q_\infty}{k^q q}\right)\right\} \end{aligned}$$

We specify the condition $\frac{dV}{dt} \geq 0$ for regions of Attractor because, as previously discussed, the system exhibits stability for all states outside the Attractor, implying that $\frac{dV}{dt} < 0$ in that region. By imposing the condition $\frac{dV}{dt} \geq 0$, within a specific domain, we can effectively constrain the attractor's boundary and systematically reduce its size relative to the state variables. This process continues until the ideal equilibrium is reached, where the attractor eventually contracts to the origin. Then, we obtained the attractor D as follows:

$$D = \{\underline{x} \in \mathbb{R}^n \mid \|\underline{x}\| \leq \max\{S_1, S_2\}\}$$
$$\text{with } S_1 = \rho^{-1}\left(\frac{\|d\|_\infty^q}{q}\right) \quad S_2 = \rho_2^{-1}\left(\frac{\|d\|_\infty^q}{k^q q}\right)$$

2.2. Design of the ISS-Based Adaptive Controller

The single-phase VSI under study is illustrated in Fig. 1. Inverter employs an H-bridge topology with an LC output filter, while the resistance of the inductor is neglected. The DC-link voltage is denoted by V_{dc}. In this paper, the load is treated as an uncertainty of the system.

The mathematical model of the VSI is obtained as follows:

$$\begin{cases} L\frac{di_L}{dt} = uV_{dc} - v_C \\ C\frac{dv_C}{dt} = i_C \end{cases} \tag{14}$$

where u is the control signal, v_c is the output voltage, i_o is the output current, and i_L, i_C are the currents through the inductor and capacitor, respectively.

By defined $\begin{cases} e_1 = v_C - v_{\text{Cref}} \\ e_2 = i_C - i_{\text{Cref}} \end{cases}$, $\underline{e} = \binom{e_1}{e_2}$, the differential relationship of tracking errors with capacitor voltage and the capacitor current is expressed as:

$$\begin{cases} \frac{de_1}{dt} = \frac{e_2}{C} \\ \frac{de_2}{dt} = \frac{-e_1}{L} + \frac{uV_{dc}}{L} + \frac{(LC\omega^2-1)v_{ref}}{L} - i_0 \end{cases} \tag{15}$$

With $H(\underline{e}) = \begin{pmatrix} 0 & \frac{V_{dc}}{L} \end{pmatrix}^T$, $G(\underline{e}) = \begin{pmatrix} 0 & -1 \end{pmatrix}^T$, and $f(\underline{e}) = \left(\frac{e_2}{C} - \frac{e_1}{L} + \frac{(LC\omega^2-1)v_{\text{ref}}}{L}\right)^T$ are three components of the system Eq. (15), as defined in Eq. (5).

During operation, the output current i_0 varies continuously, which adversely affects the performance of nonlinear controllers due to its presence in the parameter computation equations [16]. To address this issue, an ISS-based adaptive controller is employed. The complete ISS-based adaptive control design procedure for system Eq. (14) is summarized below.

Step 1: Consider e_2 as a virtual control input for the subsystem $\frac{de_1}{dt} = \frac{e_2}{C}$. Following the Lyapunov framework in [20], a candidate Lyapunov function is selected as:

$$V_1 = \frac{1}{2}Ce_1^2 \tag{16}$$

Clearly, V_1 is positive define. Its time derivative is given by:

$$\frac{dV_1}{dt} = Ce_1\frac{de_1}{dt} = e_1e_2 \tag{17}$$

To ensure GAS, the derivative $\frac{dV_1}{dt}$ must be negative definite. Accordingly, the virtual control input e_2 is designed as:

$$e_2 = r_1(e_1) = -\frac{k_1C}{k_2L}e_1, k_1, k_2 > 0 \tag{18}$$

with k_1, k_2 is the ISS-based adaptive controller parameters. By combining Equation Eq. (17) with Equation Eq. (18), it can be observed that $\frac{dV_1}{dt} = -\frac{k_1C}{k_2L}e_1^2 < 0$. Therefore, Equation Eq. (16) is positive definite and serves as a Lyapunov function, function $\frac{de_1}{dt} = \frac{e_2}{C}$ is GAS under the virtual control law defined in Eq. (18).

Step 2: From the controller for system $\frac{de_1}{dt} = \frac{e_2}{C}$ to achieve a GAS, the feedback system Eq. (15) also have a candidate Lyapunov function is selected as:

$$V = \frac{1}{2}Ce_1^2 + \frac{1}{2}(e_2 - r_1(e_1))^2 = \frac{1}{2}Ce_1^2 + \frac{1}{2}\left(e_2 + \frac{k_1C}{k_2L}e_1\right)^2 \tag{19}$$

From Eq. (19), clearly V is positive define. The time derivate of V is:

$$\frac{dV}{dt} = Ce_1\frac{de_1}{dt} + \left(e_2 + \frac{k_1C}{k_2L}e_1\right)\left(\frac{de_2}{dt} + \frac{k_1C}{k_2L}\frac{de_1}{dt}\right) \tag{20}$$

$$\begin{aligned} \frac{dV}{dt} &= -\frac{k_1C}{k_2L}e_1^2 + \left(e_2 + \frac{k_1C}{k_2L}e_1\right)(e_1 + S_3) \\ S_3 &= \frac{\left(-e_1 + (LC\omega^2 - 1)v_{ref} + uV_{dc}\right) + k_1e_2}{k_2L} \end{aligned} \tag{21}$$

For all e_1 we have $-\frac{k_1C}{k_2L}e_1^2 < 0$. To achieve GAS, $\frac{dV}{dt}$ must be negative definite. Therefore, we can choose as follows:

$$e_1 + S_3 = -\alpha\left(e_2 + \frac{k_1C}{k_2L}e_1\right), \alpha > 0 \tag{22}$$

Combine Equation Eq. (21) and Eq. (22), it can observed: $\frac{dV}{dt} = -\frac{k_1C}{k_2L}e_1^2 - \alpha\left(e_2 + \frac{k_1C}{k_2L}e_1\right)^2 < 0$. Thus, the positive definite function V is chosen as the Lyapunov function. By simplifying Equation Eq. (22), the control law $r(e)$ is obtained, which ensures GAS for system Eq. (15):

$$\begin{aligned} r(\underline{e}) = &\frac{1}{k_2V_{dc}}[+e_1(-k_2L + k_2 - \alpha k_1C) \\ &+ \left(1 - LC\omega^2\right)v_{ref} + e_2(-\alpha k_2L - k_1)] \end{aligned} \tag{23}$$

Step 3: : From Equation Eq. (19), the derivative of V with respect to $\underline{e}$ is given by:

$$\begin{aligned}\frac{\partial V}{\partial \underline{e}} &= \left(\frac{\partial V}{\partial e_1}; \frac{\partial V}{\partial e_2}\right)\\ &= \left(Ce_1 + \frac{k_1C}{k_2L}\left(e_2 + \frac{k_1C}{k_2L}e_1\right); e_2 + \frac{k_1C}{k_2L}e_1\right)\end{aligned} \tag{24}$$

Next, the controller design is finalized for the system considering external disturbances. To facilitate the derivation, the essential variables and parameters are defined based on the framework established in Section 2 as follows:

$$\begin{aligned}L_{\underline{f}}V &= \frac{\partial V}{\partial \underline{e}} f(\underline{e})\\ &= \left(Ce_1 + \frac{k_1C}{k_2L} \times S_4; S_4\right)\\ &\quad \times \begin{pmatrix} e_2/C \\ -e_1/L + (LC\omega^2 - 1)\, v_{ref}/L \end{pmatrix}\end{aligned} \tag{25}$$

With $S_4 = e_2 + \frac{k_1C}{k_2L}e_1$

$$L_{\underline{h}}V = \frac{\partial V}{\partial \underline{e}} H(\underline{e}) = \left(e_2 + \frac{k_1C}{k_2L}e_1\right)\frac{V_{dc}}{L} = \alpha(\underline{e}) \tag{26}$$

$$L_{\underline{g}}V = \frac{\partial V}{\partial \underline{e}} G(\underline{e}) = -\left(e_2 + \frac{k_1C}{k_2L}e_1\right) = c(\underline{e}) \tag{27}$$

Define $Z = \{\underline{e} \in R^n || \alpha(\underline{e}) |= 0\}$ as in Equation Eq. (11) and from Equation Eq. (26), it can be seen that:

$$Z = \left\{\underline{e} \in R^n \,\middle|\, e_2 = -\frac{k_1C}{k_2L}e_1\right\}. \tag{28}$$

The condition must be satisfied for $p = 2$ because since $\underline{e} \in \mathrm{Z}:$

$$\begin{aligned}&L_{\underline{f}}V = -\frac{k_1C}{k_2L}e_1^2, \quad L_{\underline{g}}V = 0\\ &\rightarrow L_{\underline{f}}V + \frac{1}{p}|c(e)|^p \le -\frac{k_1C}{k_2L}e_1^2 \le 0\end{aligned} \tag{29}$$

is negative define. Thus V also serves as an ISS-LF for original system, which can be controlled using the following controller, which satisfies ISS criteria:

$$u(\underline{e}) = \begin{cases} r(\underline{e}) - \frac{\left(e_2 + \frac{k_1C}{k_2L}e_1\right)L}{2V_{dc}}, & \underline{e} \notin Z \\ 0, & \underline{e} \in Z \end{cases} \tag{30}$$

with $p = 2, k = 1$.

The Attractor can be defined as follows:

$$L_{\underline{f}}V + \frac{1}{p}|c(\underline{e})|^p \le -\rho(|\underline{e}|) \rightarrow \rho(|\underline{e}|) = \frac{k_1C}{k_2L}e_1^2 \tag{31}$$

Under the following condition:

$$-W(\underline{e}) = -\frac{k_1C}{k_2L}e_1^2 - \alpha\left(e_2 + \frac{k_1C}{k_2L}e_1\right)^2 \tag{32}$$

and in conjunction with Attractor's defined method in Section 2.1, it can be inferred that the disturbance term d is bounded as follows:

$$\begin{aligned}&\|d\|_\infty^q \ge \max\{\rho(|\underline{e}|)q, W(\underline{e})k^q\}\\ &\|d\|_\infty^2 \ge \left\{2\frac{k_1C}{k_2L}e_1^2, 2\left(\frac{k_1C}{k_2L}e_1^2 + \alpha\left(e_2 + \frac{k_1C}{k_2L}e_1\right)^2\right)\right\}\end{aligned} \tag{33}$$

The Attractor D is determined as:

$$\begin{aligned}D = \{\underline{e} \in R^n \mid \|\underline{e}\| \le \max &\left\{\rho^{-1}\left(\frac{\|\underline{d}\|_\infty^q}{q}\right),\right.\\ &\left.\left.\rho_2^{-1}\left(\frac{\|\underline{d}\|_\infty^q}{k_q q}\right)\right\}\right\}\end{aligned}$$

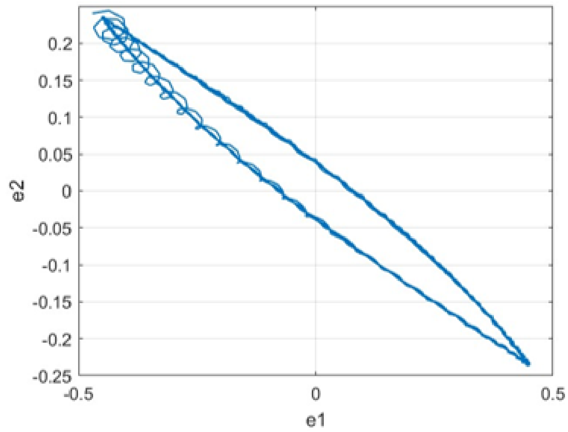

Fig. 3. Simulated Attractor of ISS-based adaptive controller

From Inequality Eq. (32) it can be observed that if $e_1 = e_2 = 0$, then the region of attraction has a radius of zero. In this case, the system becomes asymptotically stable at the equilibrium point $\underline{e} = 0$. This condition does not guarantee that the designed controller will ensure GAS at the origin; it only indicates the potential to achieve GAS. In the case where $\underline{e} \neq 0$, from the selected Lyapunov function $V = \frac{1}{2}Ce_1^2 + \frac{1}{2}\left(e_2 + \frac{k_1C}{k_2L}e_1\right)^2$, it can be observed that the region of attraction is characterized by a family of concentric ellipses centered at the origin. The maximum distance is determined by the above expression. When plotting the Attractor to validate the theoretical analysis, the results in Fig. 3 are obtained.

Attractor can be represented in a manner equivalent to a phase portrait. As discussed in Section 2.1, if there exists a Lyapunov function $V(\underline{x})$, then its time derivative must be negative outside the Attractor. This result supports the previously stated conclusion, particularly in the case where

$e_1 = e_2 = 0$, the region of attraction has a radius of zero, and the Lyapunov function's time derivative is negative outside, which means the system becomes asymptotically stable. If $\underline{e} \neq 0$, as illustrated in the Fig. 3, the system achieved GAS outside the Attractor. From Fig. 3 it can be observed that, at the initial state x_0, the trajectory lies outside Attractor, then after a certain period of time, it converges back into the Attractor around the origin. It also shows the bounderness of $\underline{e}$, with e_1 is bounded within the interval (-0.5, 0.5), while e_2 is (-0.25, 0.25). A limitation of the ISS-based adaptive controller is evident along the attractor, where driving the state variable $\underline{e}$ to 0 according to the theory becomes difficult. As a result, a residual steady-state error with respect to the reference value persists.

3. Result and discusstion

3.1. Simulation Result

MATLAB/Simulink is used to simulate the ISS-based adaptive control for VSI. In addition, simulations of the Dual-loop adaptive Lyapunov controller are conducted to provide a direct comparison between the two control strategies, thus demonstrating the advantages of the proposed controller, particularly in terms of disturbance rejection capability compared to the previously developed approach. Simulation parameters of ISS-based adaptive controller are listed in Table 1, the components are assumed to be ideal.

Table 1. Simulation parameters

Parameter	Description	Value
U_{dc}	DC bus voltage (V)	400
L_f	Filter inductance (mH)	1.3
V_{ref}	Voltage reference (V)	311
C_f	Filter capacitor (μF)	20
k_1	ISS-based adaptive controller	40
k_2	parameter	9
α	ISS Backstepping coefficient	7000

The first scenario uses an RL load to validate the conclusion from Section 2 regarding the lack of a Lyapunov stability guarantee in the previously controller.

The results shown in Fig. 4 indicate that the output voltage regulated by the ISS-based adaptive controller closely follows the voltage reference V_{ref} , whereas the Dual-loop Lyapunov-based controller exhibits unstable behavior. This contrast indicates that the Lyapunov stability claims reported in [11] are not guaranteed. Moreover, these results highlight the necessity of accounting for model uncertainties to ensure reliable stability and control performance.

The validation is further extended to a purely resistive R load, where a load step change at $t = 0.45s$ to assess

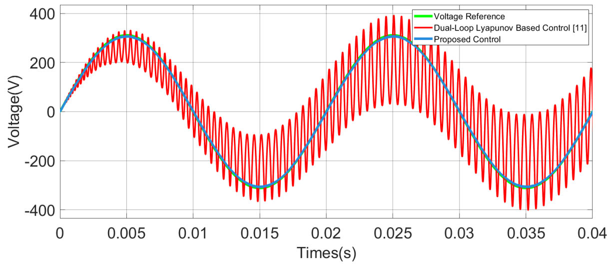

Fig. 4. Output voltage of the ISS-based adaptive controller and dual-loop Lyapunov control with RL

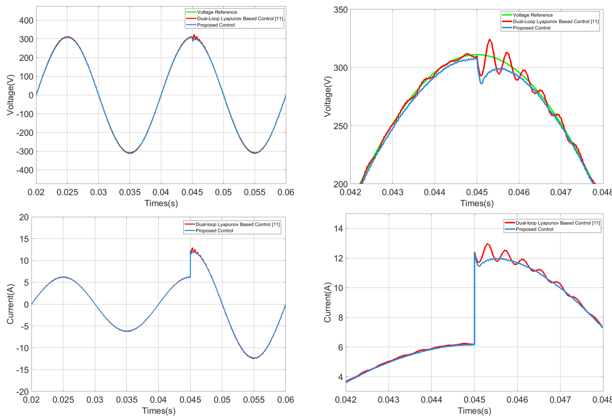

Fig. 5. Simulation results of ISS-based adaptive controller and Dual-loop Lyapunov controller [11] with R load

transient stability. The corresponding results are presented in Fig. 5. Both controllers maintain stable operation under this scenario. However, the Dual-loop Lyapunov-based controller exhibits a little overshoot during the transient period to 320.5V and undershoot to 290.3V. In contrast, the proposed ISSbased controller experiences an undershoot to 290.1V, which remains within the permissible voltage deviation range. Moreover, the ISS-based adaptive controller shows a immediate settling response, whereas the Dual-loop Lyapunov controller requires approximately 0.003s to reach steady state. These results highlight the superior transient stability performance of the proposed controller.

The next scenario uses a nonlinear bridge-rectifier load to assess controller performance and compare the disturbance rejection capabilities of the two methods. The results are shown in Fig. 6. Both controllers keep the output voltage amplitude close to the reference value, however, the Dual-loop Lyapunov controller shows larger voltage oscillations, ranging from 308V to 311V, while the ISS controller exhibits a narrower range from 307V to 308.5V. At steady state, THD for the two controllers is 1.31% and 1.4%.

A scenario is conducted to evaluate the stability of the two controllers under DC-link voltage fluctuations, where

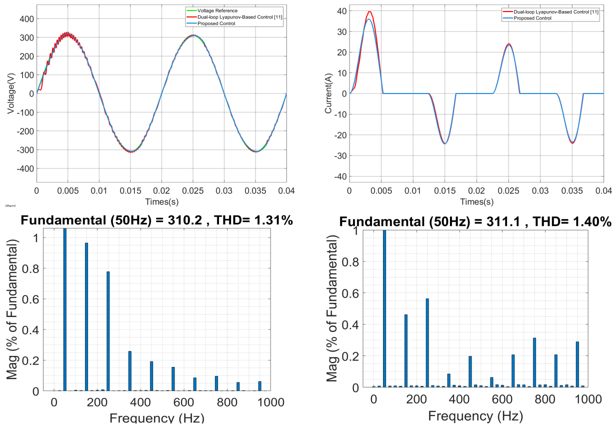

(a) (b)

Fig. 6. Simulation results of ISS-based adaptive controller and Dual-loop Lyapunov controller [11] with nonlinear load with THD of (a) ISS-based adaptive (b) Dual-loop Lyapunov [11].

the DC-link voltage decreases from $400V$ to 350 V and then returns to its nominal value.

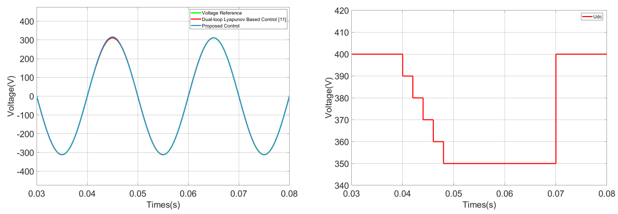

Fig. 7. Output voltage of ISS and dual-loop Lyapunov controller [11] under DC-link fluctuations.

The simulation results are presented in Fig. 7. It can be observed that at $t = 0.45$ s, the output voltage of the ISS controller remains almost unchanged and continues to accurately track v_{Cref} . In contrast, the Dual-loop Lyapunov controller exhibits a slight voltage drop of approximately 2.3 V before recovering and maintaining stable operation as the DC-link voltage returns to it's initial value.

These results show that both controllers are capable of operating stably under DC-link voltage fluctuations. Furthermore, the ISS controller exhibits superior disturbance rejection capability compared with the Dual-loop Lyapunov controller, as evidenced by its ability to maintain a more stable output voltage throughout the DC-link voltage variation process.

The results above demonstrate that the ISS-based adaptive controller performs effectively under both linear and nonlinear load conditions. In both scenarios, the output voltage exhibits a fast dynamic response, and the voltage THD meets the IEC 620403 standard (THD < 3% for linear loads, THD < 5% for nonlinear loads). Specifically, in the linear load scenario, the output voltage THD is 0.16%, while for the nonlinear load described above, the output voltage THD is 1.31%. Furthermore, no transient error is observed in the voltage at the moment of load change and DC-link voltage fluctuations.

Another important aspect to consider is the modulation index of the two methods. During the discretization process for experimental implementation, the modulation index of the Dual-loop Lyapunov controller exhibits the waveform shown in Fig. 9, which is clearly impractical and not physically realizable. In contrast, the ISS controller produces a consistent and valid control signal. Consequently, the experimental validation in this study is conducted exclusively for the ISS controller.

3.2. Experiment Results

The experimental findings are showcased to assess the dynamic response of the system and the quality of the output voltage under both linear and nonlinear loading conditions. The experimental configuration, depicted in Fig. 8, comprises a signal processing unit, the controller, and a PWM generation module implemented on a LAUNCHXL-F28379D platform from Texas Instruments. The parameters for the singlephase inverter and ISS-based adaptive controller are detailed in Table 2.

Table 2. Experiment parameters

Parameter	Description	Value
U_{dc}	DC bus voltage (V)	100
V_{ref}	Reference voltage (V)	50
L_f	Filter inductance (mH)	1.3
C_f	Filter capacitor (μF)	20
f_{sw}	Switching frequency (kHz)	10
T_s	Sampling cycle (μs)	50

The first experimental scenario is conducted to verify the stability of the proposed system under load variations. At first, the system operates with a 50Ω resistive load, and then the load resistance is reduced to 25Ω, with the results presented in Fig. 10. At the load transition instants, the output voltage exhibits transient oscillations; and stable operation is maintained after 1.2s. Before the load change, the output voltage reaches approximately $50.3V$. After the load is increased, the voltage decreases to 49.1 V , mainly due to the instantaneous drop in the DC-link voltage during the load transition. Once the DC-link voltage is restored to its nominal value, the output voltage correspondingly returns to 50.3V .

Fig. 11a presents the experimental results of the ISS-

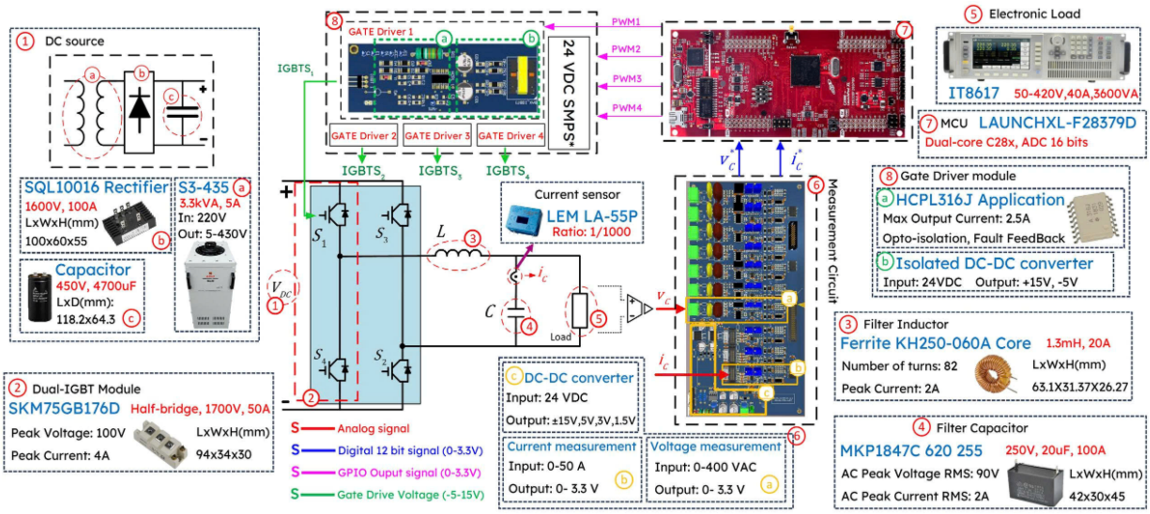

Fig. 8. Experimental system setup

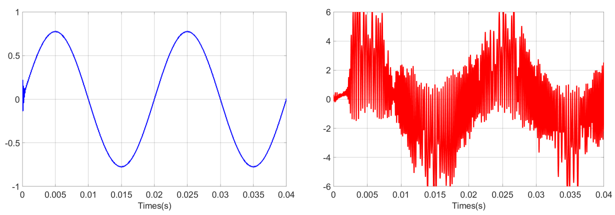

(a) (b)

Fig. 9. Modulation index of: (a) ISS-based adaptive controller; (b) Dual-loop Lyapunov controller [11]

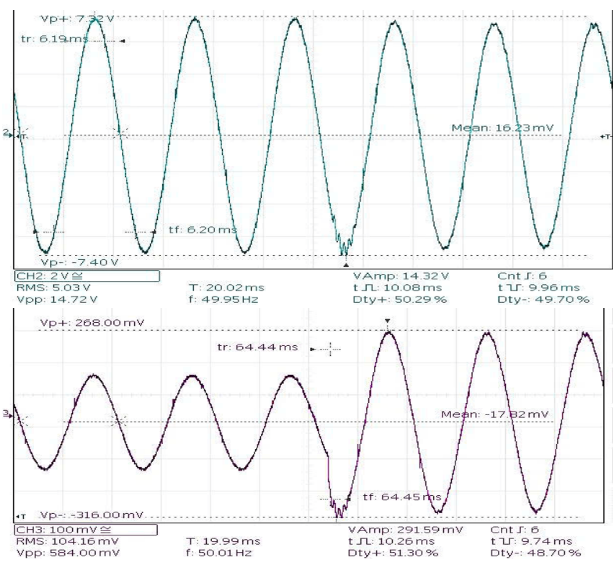

Fig. 10. Modulation index of: (a) ISS-based adaptive controller; (b) Dual-loop Lyapunov controller [11]

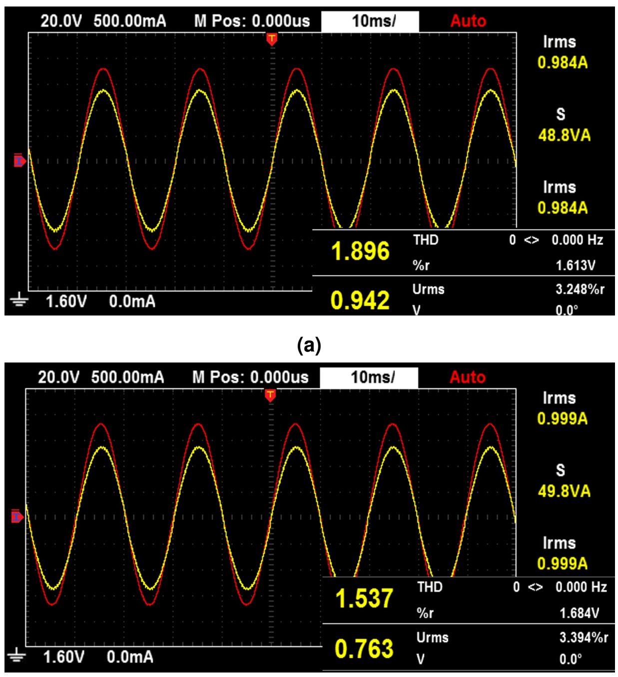

(a)

(b)

Fig. 11. Experimental results of ISS controller under load variation

based adaptive controller with a linear resistive load of $R = 50\Omega$. The measured output RMS voltage is 49.73V, corresponding to an error of 0.54%, and the output voltage THD is 1.896%, which is below 3% and thus satisfies the IEC 62040-3 standard. Fig. 11b shows the results for an RL load, which similarly meet the specified performance criteria.

Table 3. Comparison of Inverter characteristics

Parameter	[16]	[11]	This work	[12]
V_{DC}(V)	750	100	100	400
V_{AC}(V)	380	50	50	325
Controller	SMC	Dual-loop Lyapunov	ISS-based adaptive	Lyapunov + PR
f_{sw} (kHz)	9	10	10	12.5
$T_s(\mu$ s)	-	50	50	-
THD (R Load)	0.7%	-	1.896%	1.1%
THD	1.0%	-	1.324%	1.3%
(Nonlinear) t_{trans} (ms)	0.3	-	1.2	-

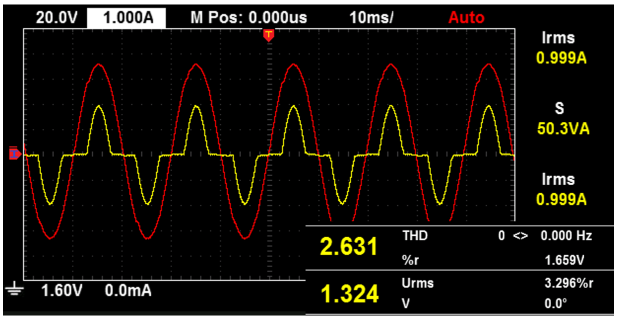

Fig. 12. Experimental results of ISS controller on the inverter with nonlinear load

Fig. 12 shows the experimental results of the ISS controller with a nonlinear load having a crest factor $CF = 2$. The measured output RMS voltage is 50.27V, corresponding to an error of 0.54% relative to the reference voltage, and the output voltage THD is 2.631%, which is below 5% and thus meets the IEC 62040-3 standard.

The comparative results are summarized in Table 3 In addition to the two above methods, the SMC scheme [16] and a Lyapunov with PR scheme [12] are included for further comparison.

4. Conclusions

This paper proposed an ISS-based adaptive control strategy for a single-phase voltage source inverter through the integration of Backstepping design and nonlinear damping theory. The developed approach aimed to improve output-voltage regulation and disturbance rejection performance under both linear and nonlinear loading conditions while maintaining a rigorous Lyapunov-based stability framework. By systematically constructing an ISS-Lyapunov function, the influence of load disturbances was effectively attenuated without requiring explicit knowledge of uncertain load parameters. Compared to conventional nonlinear approaches, particularly sliding mode control, the proposed strategy provides a mathematically consistent formulation while reducing chattering-related effects. The effectiveness of the controller was verified through both simulation and experimental studies, demonstrating stable inverter operation, low output-voltage distortion, and satisfactory transient response under load variations and nonlinear disturbances. Nevertheless, due to the attractor property of the ISS framework, the associated state variable may not converge exactly to zero, resulting in a small residual steady-state tracking error. Future work will focus on improving steady-state performance under more complex and uncertain operating conditions.

Acknowledgment

This research is funded by Hanoi University of Science and Technology (HUST) under project number T2024-TĐ-012.

References

[1] M. Li, Y. Gui, Y. Guan, J. Matas, J. M. Guerrero, and J. C. Vasquez, (2021) *"Inverter Parallelization for an Islanded Microgrid Using the Hopf Oscillator Controller Approach With Self-Synchronization Capabilities"* **IEEE Transactions on Industrial Electronics** *68*(11): 10879–10889. DOI: 10.1109/TIE.2020.3031520.

[2] N. Abdel-Rahim and J. Quaicoe, (1996) *"Analysis and design of a multiple feedback loop control strategy for single-phase voltage-source UPS inverters"* **IEEE Transactions on Power Electronics** *11*(4): 532–541. DOI: 10.1109/63.506118.

[3] H. Rezazadeh, M. Monfared, M. Fazeli, and S. Golestan. "Single-phase Grid-forming Inverters: A Review". In: *2023 International Conference on Computing, Electronics & Communications Engineering (iCCECE)*. 2023, 7–10. DOI: 10.1109/iCCECE59400.2023.10238661.

[4] M. Blachuta, Z. Rymarski, R. Bieda, K. Bernacki, and R. Grygiel. "Design, Modeling and Simulation of PID Control for DC/AC Inverters". In: *2019 24th International Conference on Methods and Models in Au-*

tomation and Robotics (MMAR). 2019, 428–433. DOI: 10.1109/MMAR.2019.8864609.

[5] R. Wu, X. Zhang, and W. Jiang, (2025) *"Bifurcation analysis and control in a DC–AC inverter with PID controller"* **International Journal of Circuit Theory and Applications** *53*(4): 2125–2153. DOI: https://doi.org/10.1002/cta.4209. eprint: https://onlinelibrary.wiley.com/doi/pdf/10.1002/cta.4209. URL: https://onlinelibrary.wiley.com/doi/abs/10.1002/cta.4209.

[6] H. Komurcugil, N. Altin, S. Ozdemir, and I. Sefa, (2016) *"Lyapunov-Function and Proportional-Resonant-Based Control Strategy for Single-Phase Grid-Connected VSI With LCL Filter"* **IEEE Transactions on Industrial Electronics** *63*(5): 2838–2849. DOI: 10.1109/TIE.2015.2510984.

[7] A. Cherifi, A. Chouder, A. Kessal, A. Hadjkaddour, A. Aillane, and K. Louassaa. "Control of a Voltage Source Inverter in a Microgrid Architecture using PI and PR Controllers". In: *2022 19th International Multi-Conference on Systems, Signals & Devices (SSD)*. 2022, 1471–1477. DOI: 10.1109/SSD54932.2022.9955891.

[8] M. Tahmid Wara Ucchas, M. Mustafiz Nuhas, M. Toufiquzzaman, A. Jaber Mahmud, and M. Fokhrul Islam. "Performance and Comparative Analysis of PI and PID Controller-based Single Phase PWM Inverter Using MATLAB Simulink for Variable Voltage". In: *2022 Second International Conference on Advances in Electrical, Computing, Communication and Sustainable Technologies (ICAECT)*. 2022, 1–6. DOI: 10.1109/ICAECT54875.2022.9807857.

[9] S. Li, J. Yang, W.-H. Chen, and X. Chen. "Disturbance Observer-Based Control: Methods and Applications". In: Boca Raton, FL: CRC Press, 2016. Chap. 3. DOI: 10.1201/b16570.

[10] E. Sariyildiz and K. Ohnishi. "Robust stability anaylsis of the system with disturbance observer: The real parametric uncertainity approach I". In: *2012 IEEE International Conference on Mechatronics and Automation*. 2012, 1779–1784. DOI: 10.1109/ICMA.2012.6285091.

[11] X. Zhang, J. He, H. Ma, Z. Ma, and X. Ge. "An Adaptive Dual-loop Lyapunov-Based Control Scheme for a Single-Phase Stand-Alone Inverter to Improve Its Large-Signal Stability". In: *Stability Enhancement Methods of Inverters Based on Lyapunov Function, Predictive Control, and Reinforcement Learning*. Singapore: Springer Nature Singapore, 2023. Chap. 3, 33–46. DOI: 10.1007/978-981-19-7191-4_3.

[12] H. Komurcugil, N. Altin, S. Ozdemir, and I. Sefa, (2015) *"An Extended Lyapunov-Function-Based Control Strategy for Single-Phase UPS Inverters"* **IEEE Transactions on Power Electronics** *30*(7): 3976–3983. DOI: 10.1109/TPEL.2014.2347396.

[13] H. Komurcugil, S. Biricik, S. Bayhan, and Z. Zhang, (2021) *"Sliding Mode Control: Overview of Its Applications in Power Converters"* **IEEE Industrial Electronics Magazine** *15*(1): 40–49. DOI: 10.1109/MIE.2020.2986165.

[14] X. Yu, Y. Feng, and Z. Man, (2021) *"Terminal Sliding Mode Control – An Overview"* **IEEE Open Journal of the Industrial Electronics Society** *2*: 36–52. DOI: 10.1109/OJIES.2020.3040412.

[15] J. Samantaray and S. Chakrabarty. "Discrete Time Sliding Mode Control". In: *Control Theory in Engineering*. Ed. by C. Voloşencu, A. Saghafinia, X. Du, and S. Chakrabarty. London, UK: IntechOpen, 2020. Chap. 5. DOI: 10.5772/intechopen.91245. URL: https://doi.org/10.5772/intechopen.91245.

[16] L. Zheng, F. Jiang, J. Song, Y. Gao, and M. Tian, (2018) *"A Discrete-Time Repetitive Sliding Mode Control for Voltage Source Inverters"* **IEEE Journal of Emerging and Selected Topics in Power Electronics** *6*(3): 1553–1566. DOI: 10.1109/JESTPE.2017.2781701.

[17] W. Gao, Y. Wang, and A. Homaifa, (1995) *"Discrete-time variable structure control systems"* **IEEE Transactions on Industrial Electronics** *42*(2): 117–122. DOI: 10.1109/41.370376.

[18] H. Pinheiro, A. Martins, and J. Pinheiro. "A sliding mode controller in single phase voltage source inverters". In: *Proceedings of IECON'94 - 20th Annual Conference of IEEE Industrial Electronics*. ***1***. 1994, 394–398 vol.1. DOI: 10.1109/IECON.1994.397810.

[19] E. D. Sontag. "Input to State Stability: Basic Concepts and Results". In: *Nonlinear and Optimal Control Theory*. Ed. by P. Nistri and G. Stefani. ***1932***. Lecture Notes in Mathematics. Berlin, Heidelberg: Springer, 2008, 163–220. DOI: 10.1007/978-3-540-77653-6_3.

[20] A. Aleksandrov, D. Efimov, and S. Dashkovskiy, (2023) *"Design of finite-/fixed-time ISS-Lyapunov functions for mechanical systems"* **Mathematics of Control, Signals, and Systems** *35*(1): 1–29. DOI: 10.1007/s00498-022-00338-x.

[21] E. D. Sontag, (1989) *"A 'universal' construction of Artstein's theorem on nonlinear stabilization"* **Systems & Control Letters** ***13***(2): 117–123. DOI: https://doi.org/10.1016/0167-6911(89)90028-5. URL: https://www.sciencedirect.com/science/article/pii/0167691189900285.

[22] E. D. Sontag and Y. Wang, (1995) *"On characterizations of the input-to-state stability property"* **Systems & Control Letters** ***24***(5): 351–359. DOI: https://doi.org/10.1016/0167-6911(94)00050-6. URL: https://www.sciencedirect.com/science/article/pii/0167691194000506.

[23] E. D. Sontag, (1995) *"On the Input-to-State Stability Property"* **European Journal of Control** ***1***(1): 24–36. DOI: https://doi.org/10.1016/S0947-3580(95)70005-X. URL: https://www.sciencedirect.com/science/article/pii/S094735809570005X.

[24] Y. Lin, E. D. Sontag, and Y. Wang, (1996) *"A Smooth Converse Lyapunov Theorem for Robust Stability"* **SIAM Journal on Control and Optimization** ***34***(1): 124–160. DOI: 10.1137/S0363012993259981. URL: https://doi.org/10.1137/S0363012993259981.

[25] E. Kolbasi and M. Seker. "Nonlinear robust backstepping control method approach for single phase inverter". In: *2016 21st International Conference on Methods and Models in Automation and Robotics (MMAR)*. 2016, 954–958. DOI: 10.1109/MMAR.2016.7575266.

[26] A. Latif, L. Khan, and S. Ahmad. "Nonlinear Backstepping Based Control of Single-phase Inverter in a Standalone Photovoltaic System". In: *2021 International Bhurban Conference on Applied Sciences and Technologies (IBCAST)*. 2021, 636–641. DOI: 10.1109/IBCAST51254.2021.9393189.

[27] O. Diouri, N. Es-Sbai, F. Errahimi, A. Gaga, and C. Alaoui. "Control of single phase inverter using backstepping in stand-alone mode". In: *2019 International Conference on Wireless Technologies, Embedded and Intelligent Systems (WITS)*. 2019, 1–6. DOI: 10.1109/WITS.2019.8723761.

[28] P. Vu, Q. Nguyen, M. Tran, G. Todeschini, and S. Santoso, (2018) *"Adaptive backstepping approach for dc-side controllers of Z-source inverters in grid-tied PV system applications"* **IET Power Electronics** ***11***(14): 2346–2354. DOI: https://doi.org/10.1049/iet-pel.2018.5763. URL: https://ietresearch.onlinelibrary.wiley.com/doi/abs/10.1049/iet-pel.2018.5763.

[29] M. Krstic, I. Kanellakopoulos, and P. V. Kokotovic. *Nonlinear and Adaptive Control Design*. New York: John Wiley & Sons, 1995. Chap. 2, 21–86. URL: https://dl.acm.org/doi/abs/10.5555/546475.

[30] R. A. Freeman and P. V. Kokotovic. *Robust Nonlinear Control Design: State-Space and Lyapunov Techniques*. Boston, MA: Birkhäuser Boston, 1996. Chap. 3, 15–32. DOI: 10.1007/978-0-8176-4759-9.

[31] H. K. Khalil. *Nonlinear Systems*. New York: Macmillan Publishing Company, 1992. Chap. 4. URL: https://files.dooctly.com/samples/solution-manual-nonlinear-systems-3e-khalil.pdf.